Atmos. Chem. Phys. Discuss., 12, 12391–12421, 2012
www.atmos-chem-phys-discuss.net/12/12391/2012/
doi:10.5194/acpd-12-12391-2012

Atmospheric Chemistry and Physics Discussions

Relationships among Brewer-Dobson circulation, double tropopauses, ozone and stratospheric water vapour

J. M. Castanheira[1], **T. R. Peevey**[2,3], **C. A. F. Marques**[1], **and M. A. Olsen**[4]

[1]CESAM, Department of Physics, University of Aveiro, Portugal
[2]National Center for Atmospheric Research, Boulder, Colorado, USA
[3]Center for Limb Atmospheric Sounding, University of Colorado at Boulder, Boulder, Colorado, USA
[4]Goddard Earth Sciences Technology and Research, Morgan State University, Baltimore, Maryland, USA

Received: 31 March 2012 – Accepted: 30 April 2012 – Published: 15 May 2012

Correspondence to: J. M. Castanheira (jcast@ua.pt)

Published by Copernicus Publications on behalf of the European Geosciences Union.

Abstract

The statistical relationships among the variability of the area covered by double tropopause (DT) events, the strength of the tropical upwelling, the variabilities of total column ozone and of lower stratospheric water vapour are analyzed. The QBO and ENSO signals in the double tropopause and tropical upwelling as well as their influence on the statistical relationships are also presented. The analysis is based on both reanalysed data (ERA-Interim) and satellite data.

Significant anticorrelations were found between the area covered by double tropopause events and the total column ozone in the midlatitudes of the Northern Hemisphere. This relationship is confirmed by a large positive correlation between the areas covered by ozone laminae and double tropopause events as found in the HIRDLS satellite data. Significant anticorrelations were also found between the global area of double tropopause events and the near global (50° S–50° N) water vapour in the lower stratosphere.

The correlations of DT variables with total column ozone and ozone laminae are both consistent with the poleward displacement of tropical air with lower ozone mixing ratio and with tropospheric intrusions of tropical tropospheric air into the lower extratropical stratosphere.

Finally, a significant anticorrelation was found between the tropical upwelling and the near global lower stratospheric water vapour. The step like decrease in the lower stratospheric water vapour after 2001 is mirrored by a step like increase in the tropical upwelling.

1 Introduction

The distribution of ozone and water vapour in the stratosphere strongly impacts the radiative heating field and the stratospheric dynamics. Stratospheric ozone accounts for about 90 % of the total column ozone and controls the amount of damaging UV

ACPD
12, 12391–12421, 2012

radiation reaching the earth surface. Water vapour with its associated feedbacks is the main radiative driver of the climate system, and, recently, Solomon et al. (2010) showed that stratospheric water vapour fluctuations may modulate the decadal global surface warming. Stratospheric dynamics have been shown to be important for long range weather forecasts and climate (e.g., Roff et al., 2011; Sigmond et al., 2008, and references therein).

Water vapour enters in the stratosphere through the tropical tropopause (Mote et al., 1996). It is transported poleward by the Brewer-Dobson Circulation (BDC) and by quasi-horizontal mixing (e.g., Bönisch et al., 2011, and references therein). It is difficult to separate the contribution of these two transport processes because both the residual circulation and mixing are the result of wave breaking. However, a detailed understanding of the two contributions is required to assess how well climate models simulate stratospheric dynamics and tracer transport, and to increase the confidence in their projections.

Castanheira and Gimeno (2011) and Peevey et al. (2012) showed that double tropopause events (DTs) are associated with Rossby waves in the subtropics and midlatitudes. These waves can produce intrusions of tropical tropospheric air into the extratropical lower stratosphere (Randel et al., 2007; Pan et al., 2009). If these waves break they will contribute to the exchange of trace gases between the troposphere and the stratosphere through irreversible mixing. It is reasonable to expect that the variability in the frequency of double tropopause events will reflect variability in the Rossby wave activity. Changes in the subtropical wave activity may ultimately be associated with changes in the tropical upwelling. Guided by such possible links, this study will show statistical relationships among the BDC, double tropopauses, ozone and stratospheric water vapour, based on reanalyzed and instrumental data. The obtained relationships are expected to increase our understanding of the meridional transport of trace gases.

ACPD
12, 12391–12421, 2012

2 Data and method

The present study is based on the ERA Interim (ERA-I) reanalysis data (Dee et al., 2011) on isobaric levels at 00:00 and 12:00 UT from 1979 to 2010, on the total column ozone observed from three satellite instruments (Earth Probe, Nimbus 7 and OMI), and on water vapour data from the HALOE and Aura MLS. The water vapour data were kindly made available by Dr. William Randel and are the same used in Randel (2010). An independent assessment of the relationship between ozone and DTs was done using observations by the High Resolution Dynamics Limb Sounder (HIRDLS) satellite instrument.

The first and, if present, second thermal lapse rate tropopauses were identified using the conventional WMO criterion:

(a) The *first tropopause* is defined as the lowest level at which the lapse rate decreases to 2 K km^{-1} or less, provided also that the average lapse rate between this level and all higher levels within 2 km does not exceed 2 K km^{-1}.

(b) If above the first tropopause the average lapse rate between any level and all higher levels within 1 km exceeds 3 K km^{-1} then a *second tropopause* is defined by the same criterion as in (a). This tropopause may be either within or above the 1 km layer.

Because of the low (∼ 1 km) vertical resolution in the UTLS, condition (b) in the above definition was reduced to 2.5 K km^{-1} when analyzing the ERA-I data. A similar procedure was applied by Randel et al. (2007), who reduced condition (b) to 2 K km^{-1} in their analysis of the ERA40 data. The criteria used to find the tropopauses were applied using an algorithm that is similar to that used by Birner (2010) (which in turn is a slight variation of the algorithm used by Reichler et al., 2003).

For each reanalysis time we calculated the fraction of area (FA_{NH}) of the latitudinal band 20–65° N, where double tropopause (DT) events occur. A similar time series, FA_{SH}, was obtained for the latitudinal band 20–65° S. Monthly means were

ACPD
12, 12391–12421, 2012

then calculated. Time series of monthly mean anomalies were obtained by subtracting the interannual mean of each calendar month. The mean of the two time series [FA = (FA_{NH}+FA_{SH})/2] represents the fraction of area of the two latitudinal bands where DTs occur.

Figure 1 shows a 5-month running average of the anomalies of FA. The figure also shows the multilinear regression of the FA anomalies onto time series of the QBO, ENSO and solar cycle. The QBO is represented by the monthly mean of the equatorial zonal mean zonal wind at 30 and 70 hPa. These two time series are nearly orthogonal (their correlation is $r = -0.08$), and allow to account for the strength and phase of the QBO. The ENSO is represented by the Multivariate ENSO Index (MEI) from the NOAA website (http://www.esrl.noaa.gov/psd/enso/mei/). The solar cycle is represented by the adjusted time series of the solar 10.7 cm flux observed in Penticton, British Columbia, available at http://www.ngdc.noaa.gov/stp/solar/flux.html. All indices are available with a (calendar) monthly mean time resolution and a 5-month running average was applied before the multilinear regression was performed. The area associated with DT events does not show any correlation ($r = -0.05$) with the solar cycle, whereas the correlation values with the ENSO index and the QBO are $r = -0.40$ and $|r| = 0.50$, respectively. The multilinear regression coefficients show that DTs events are more frequent during the easterly phase of the QBO at 70 hPa. Because the relationships among BDC, double tropopauses, ozone and stratospheric water vapour may be sensitive to the phases of ENSO and the QBO, we performed the calculations for both the total data anomalies and for the time series with the signals of the QBO, ENSO and solar cycle removed using a multilinear regression.

Ozone and water vapour were available as (calendar) monthly means. Other variables with hourly resolution were averaged into calendar monthly means. The seasonal cycle of each variable was removed by subtracting the interannual monthly mean from each month. The anomalies were then smoothed by a 5-month running mean. Because the short length of the ozone time series from the Earth Probe and OMI instruments, all time series used in the analysis of the relationships with ozone were smoothed

ACPD
12, 12391–12421, 2012

by a 3-month running mean to maintain an adequate number of statistical degrees of freedom. The treatment of the HIRDLS data will be explained in next section.

The statistical significance of correlations between time series which were smoothed by 5-month running means and the statistical significance of correlations between time series which were smoothed by 3-month running means were assessed adopting the conservative assumption that only 2 and 3 degrees of freedom per year remained after the smoothing, respectively. A two-sided parametric test was considered for all cases.

3 Results

3.1 Ozone versus DTs

Randel et al. (2007), Pan et al. (2009) and Castanheira and Gimeno (2011) showed observational evidence that double tropopause structures could result from excursions of the tropical tropopause and tropical air over the extratropical tropopause. In the lower stratosphere, ozone mixing ratios are poleward increasing from the tropics to extratropics so large positive anomalies in the area associated with DTs should be associated with negative anomalies of the zonal mean ozone in the lower extratropical stratosphere. Because much of total column ozone is concentrated in the lower stratosphere, we expect the signal of DTs also to be detectable in the total ozone.

Castanheira and Gimeno (2011) and Peevey et al. (2012) showed that the variability of the meridional extension of the tropical tropopause over the extratropical tropopause, and therefore the variability of the area where DTs occur, is associated with Rossby wave variability. Such waves may be reversible, with tropical air moving to the extratropics and returning back the tropics without mixing into the midlatitudes. Higher correlation between the fractional area of DTs and the total column ozone is expected, if we define ozone time series given by the weighted area average of total column ozone, in the extratropical latitudinal band where the occurrence of DTs is more frequent. Figure 1 of Castanheira and Gimeno (2011) shows that the maximum frequency of DT

ACPD
12, 12391–12421, 2012

events occurs in the latitudinal band 30–45° N. Although, Fig. 1 of Castanheira and Gimeno (2011) shows results for the NH winter, a similar result is obtained considering the full year. Therefore, ozone time series were constructed using the area weighted averages of column ozone anomalies within the previously mentioned latitudinal band (30–45° N). Figure 2 shows a scatter plot of the mean ozone anomalies as a function of area anomaly of DTs in the NH (FA_{NH}). The plot shows significant anticorrelation between the anomalies of total ozone and the area of DTs. The correlations values are $r = -0.74$, -0.66 and -0.74 for the ozone data derived from the Earth Probe, Nimbus 7 and OMI satellites instruments, respectively. Figure 3 shows a similar plot but for the ozone column from the ERA-I reanalysis (1979–2010). The correlation value is $r = -0.61$. In order to reduce the possible effects associated with chemical ozone depletion, the time series of Nimbus 7 (1979–1992) was linearly detrended, and a 5-yr running mean was removed from the ozone series derived from the ERA-I reanalysis. The correlation for OMI data is statistically significant at the 95 % level, and the correlations for Earth Probe, Nimbus 7 and ERA-I data are statistically significant above the 99 % level.

The relationship between ozone and DTs was tested independently by using variables derived from the HIRDLS instrument data for the period 2005–2007. The analysed variables were the areas associated with ozone laminae and DTs in the NH. Ozone lamina are identified following the method of Olsen et al. (2010). However, we do not restrict the lamina thickness nor require continuity across adjacent profiles as originally presented by Olsen et al. (2010). In addition, the vertical range is expanded, spanning 340 K to 550 K on 5 K increment potential temperature surfaces. For consistency with the method of ozone lamina identification, HIRDLS temperature profiles were averaged within 2 degree latitude bins between 22°–72° N, and the DTs were identified as in Peevey et al. (2012). Next, two daily time series representing the areas of DTs and ozone laminas were calculated. The areas of each ozone lamina profile and each DT profile are represented by the cosines of the latitude of bins where they are found. Daily time series for both the areas of the laminae and DTs are then calcu-

ACPD
12, 12391–12421, 2012

lated by a sum of the cosines of the latitudes of all bins where laminae or DTs were found each day. During this process two restrictions were implemented: (1) the second tropopause must be between 70 hPa and 150 hPa and (2) the potential temperature of the ozone minimum is below the maximum potential temperature of the restricted second tropopause or below 400 K if no second tropopause is present. This helps to ensure that both the DT and ozone lamina are characteristic of a tropospheric intrusions. We deseasonalize the time series by first finding the average area for each day of the year and smoothing using a 29-day moving average. That time series, which represents the seasonal cycle, is removed from the original data. This is done for both the DT and ozone lamina area time series. The anomaly time series were then smoothed by a 5-day running mean. Additionally, because both DT and ozone laminae frequency are small during the summer (Olsen et al., 2010; Peevey et al., 2012), only anomalies between November and June were analyzed. As seen in Fig. 4, there is a strong correlation between the area of DTs and the area of ozone laminae. This is consistent with negative anomalies of total column ozone associated with positive anomalies in the area of DTs due to both the northward displacement of tropical air with low ozone mixing ratio and tropospheric intrusions of tropical tropospheric air into the lower extratropical stratosphere. Again, using a very conservative assumption that there are only three degrees of freedom per month and a two-sided test, the correlation between ozone laminae and DTs is statistically significant above the 99 % level.

3.2 Lower stratospheric water vapour versus DTs

If waves associated with the tropopausal overlap have large amplitudes, they may break resulting in a mixing of tropical and extratropical air (Pan et al., 2009), contributing for the exchange of trace gases between the tropics and extratropics. Bönisch et al. (2011) suggested that the stratospheric water vapour drop after the year 2001 was a consequence of an enhanced quasi-horizontal (isentropic) mixing accompanied by an intensification of the residual circulation in the lower most stratosphere (LMS).

ACPD
12, 12391–12421, 2012

Considering the above and assuming that large anomalies in the FA time series for DTs may be associated with quasi-horizontal mixing events in the LMS, we analyzed the correlation between FA and the mixing ratio of water vapour on isobaric levels. Figure 5 shows these correlations with a time series of near global (50° S–50° N) water vapour data derived from the HALOE and Aura MLS instruments. There is a significant (above the 99 % level) anticorrelation between FA and the stratospheric mixing ratio in the lower stratosphere. The anticorrelation is found both in the total variability and the residual variability, i.e., with the variability associated with the QBO, ENSO and solar cycle removed from the time series using a multilinear regression. The large variation of the correlations below the 200-hPa level are likely due to the small number of observations there. Similar correlation curves were obtained using water vapour from ERA-I reanalysis (Fig. 6). Maximum anticorrelations are found at the 150-hPa level (more clear in Fig. 6). The occurrence of maximum anticorrelation, at such a low level, may be due to subsidence of the first tropopause associated with DT events (Añel et al., 2008; Peevey et al., 2012). Because water vapour mixing ratio drops vary rapidly through the tropopause layer, the subsidence will induce large negative anomalies in the water vapour mixing ratio at fixed isobaric level near the tropopause.

ERA-I water vapour analysis at stratospheric levels has very little influence from observations being mostly a model field product (Dee et al., 2011). A comparison of Figs. 5 and 6 suggests that the two water vapour time series do not capture the same variability. For the satellite observations, in the lower stratosphere between 100- and 20-hPa, we note that the magnitudes of the correlation coefficients considering all variability are smaller than those for the residual variability, whereas for the ERA-I the magnitudes of the correlation coefficients considering all variability are greater than those for the residual variability.

3.3 Tropical upwelling versus water vapour and DTs

The main sources of stratospheric water vapour are methane oxidation and transport from the troposphere through the tropical tropopause. This implies that variability and

ACPD
12, 12391–12421, 2012

trends in the stratospheric water vapour field may be caused by changes in the fraction of oxidised methane (Le Texier et al., 1988) and changes in the entry mixing ratios of methane and water vapour as well as by their transport associated with the diabatic meridional circulation, i.e. the Brewer-Dobson circulation, and the irreversible quasi-horizontal mixing (Mote et al., 1996). In this section, the variability of the near global lower stratospheric water vapour will be related to the variability in the upwelling through the tropical tropopause which is placed near 100-hPa.

The ERA-I mean residual vertical velocity, $\langle\overline{w}^*\rangle$, in the tropical region bounded by the latitudes $-\phi_0$ and ϕ_0, was computed using the downward control principle as in Randel et al. (2002):

$$\langle\overline{w}^*\rangle(z) = \frac{1}{2\rho_0(z)\sin\phi_0}\left\{\int_z^\infty\left[\cos\phi\,\frac{\nabla\cdot\mathbf{F}-\rho_0(z')\partial\overline{m}/\partial t}{\partial\overline{m}/\partial\phi}\right]_{\overline{m}}\mathrm{d}z'\right\}_{-\phi_0}^{\phi_0}, \quad (1)$$

where z is the log-pressure altitude, $\rho_0(z) = \rho_s e^{-z/H}$ is the reference density, $\mathbf{F}$ is the Eliassen-Palm (E-P) flux, $\overline{m} = a\cos\phi(\overline{u}+a\Omega\cos\phi)$ is the zonal mean absolute angular momentum. All variables were defined as in Sect. 3.5 of Andrews et al. (1987), and the subscript $\overline{m}$ means that the integral was evaluated along contours of constant angular momentum, $\overline{m}(\phi,\ z)$. In this study, the residual velocity was calculated at the log pressure altitude of the 100-hPa level.

In the remaining analysis, results will be shown for the mean residual velocity within the tropical band 22.5° S–22.5° N. For wider tropical bands the results remain qualitatively the same. On the other hand, for smaller latitude limits, the calculation of the integral along contours of constant $\overline{m}(\phi,\ z)$ is problematic because the condition $\partial\overline{m}/\partial\phi \neq 0$ is violated a large number of times.

ACPD
12, 12391–12421, 2012

3.3.1 Tropical upwelling versus DTs and QBO

The residual velocity is forced by the E-P flux divergence, which, in the linear quasi-geostrophic approximation, is proportional to wave activity. Because of this relationship and the association of double tropopauses with Rossby waves, it is reasonable to expect a relationship between the residual velocity in the lower stratosphere and the area covered by double tropopauses. As seen in Fig. 7, a strong linear relationship exists between DTs and the vertical residual velocity at the tropopause level. Moreover, the curves in Fig. 8 show that the relationship between DTs and the vertical residual velocity is intrinsic to them and not due to "external" factors like the QBO, the ENSO or the solar cycle.

The results of the correlations between the residual velocity and the QBO, the ENSO and the solar flux showed that there is no significant correlation with the ENSO and $\langle \overline{w}^* \rangle$ ($r = 0.03$) and no significant correlation with the solar flux and $\langle \overline{w}^* \rangle$ ($r = -0.03$). On the other hand, there is a strong correlation ($|r| = 0.63$) between the QBO and $\langle \overline{w}^* \rangle$. As referred in the data section, the time series of the equatorial zonal mean zonal wind at 30 and 70 hPa, used to represent the QBO, are nearly orthogonal. The single correlations of $\langle \overline{w}^* \rangle$ with the equatorial zonal mean zonal wind at 30 and 70 hPa are $r = 0.05$ and $r = -0.63$, respectively. These results indicate that, in the mean, the residual velocity is stronger during the easterly phase of the QBO at 70 hPa.

3.3.2 Tropical upwelling versus water vapour

As suggested at the end of Sect. 3.2, the time series of water vapour derived from the ERA-I reanalysis and derived from the HALOE and Aura MLS instruments do not capture the same variabilities. Figures 9 and 10 show the correlations between the residual vertical velocity, at 100-hPa, and the near global water vapour at several isobaric levels. Because the residual velocity is associated with the flux of humidity into the stratosphere, its time series leads the time series of lower stratospheric water vapour. We found that a leading period of five months maximizes the correlations.

ACPD
12, 12391–12421, 2012

Compared to the correlations obtained for the DTs (see Fig. 6), the correlation between the ERA-I water vapour and the tropical upwelling shown in Fig. 9 are much smaller in the lower stratosphere. The values of the correlation for the residual variabilities fluctuate around zero, indicating that they are not statistical significant. Therefore, the correlation of the ERA-I water vapour with the DTs must be due to the subsidence of the first tropopause during DT events (Añel et al., 2008; Peevey et al., 2012), and to the poleward advection of air with low water vapour mixing ratio found above the tropical cold point tropopause. In this respect, we note that the minimum specific humidity in the lower most stratosphere in the tropics, due to the cold temperature observed there (see, for example, Fig. 2a, b of Oman et al., 2008) is well captured in the reanalysis (not shown). On the other hand, Fig. 10 shows strong correlation between the water vapour derived from the HALOE and Aura MLS instruments and the tropical upwelling. In the lower stratosphere, above 150-hPa, the correlation is higher than the correlation with DTs. These results confirm that the time series of water vapour derived from the ERA-I reanalysis and derived from the HALOE and Aura MLS instruments do not capture the same variabilities. The ERA-I time series miss a large fraction of the variability due to the tropical upwelling.

The large correlation between the tropical upwelling and the fraction of area covered with DTs, and the large correlation between tropical upwelling and water vapour in satellite data may indicate that much of the water vapour and DTs correlated variabilities are also covariant with the tropical upwelling. The differences between the red and blue curves in Fig. 11 show that such an association is in fact true. The blue curve shows that the correlations between the DT and water vapour time series, in the lower most stratosphere, are strongly reduced when we subtract the variability regressed on the tropical upwelling time series. This result shows that it is difficult untangle the effects due to the transport by the residual circulation and to the quasi-horizontal motion in the observed data (Bönisch et al., 2011). Mote et al. (1996) showed that the variability of the tropical upwelling is a determinant for the variability of lower stratospheric water vapour. The results of the present study obtained with the ERA-I reanalysis show that

ACPD
12, 12391–12421, 2012

the quasi-horizontal motion in the lower most stratosphere is also important. Figures 9 and 12 show a small relationship between the variability of ERA-I water vapour, in the lower stratosphere, and tropical upwelling. As already mentioned, this are likely due to the fact that ERA-I water vapour analysis at stratospheric levels has very little influence from observations being mostly a model field product (Dee et al., 2011). However, the results show that, at least in the model variability, there is a clear relationship between the variabilities of ERA-I water vapour and DTs, which are associated with horizontal motions.

A step like decrease of water vapour in the lower stratosphere after 2001 has been analyzed in the recent literature (e.g. Randel et al., 2006; Randel, 2010). Given the strong correlation between tropical upwelling and water vapour in satellite data, if the observed decrease in stratospheric water vapour after 2001 was due to a change in the transport through the tropical tropopause as argued by Randel et al. (2006) and by Randel (2010), then a clear signal should be also visible in the time series of the tropical upwelling. Figure 13 shows an increase in the mean tropical upwelling (upward branch of the BDC) after 2001. Moreover, Fig. 14 shows that the increase is not covariant with the QBO, the ENSO or the solar cycle. This increase of the mean tropical upwelling is consistent with a higher, colder and drier tropical tropopause leading to a decrease of water vapour in the lower stratosphere (Randel, 2010, his Fig. 13).

4 Concluding remarks

This study presents a statistical analysis of the relationships among the upward branch of the BDC (tropical upwelling), the area covered by DTs, the ozone and the lower stratospheric water vapour. The influence of the QBO and the ENSO signals on the relationships was also assessed. A clear signal of the QBO and the ENSO on the frequency of DTs is demonstrated. The strong correlation between the strength of the upward branch of the BDC as determined by the downward control principle and the

ACPD
12, 12391–12421, 2012

area of DTs is consistent with the findings of Castanheira and Gimeno (2011) and Peevey et al. (2012) that show an association between DTs and Rossby waves.

The negative correlations between the area covered by DTs and the total column ozone or the lower stratospheric water vapour may be understood as a consequence of the poleward displacement of the tropical air in the upper troposphere/lower stratosphere (UTLS). This is likely the case because the lower tropical stratosphere is drier and has smaller ozone mixing ratios, therefore, the poleward displacement of tropical UTLS air will produce negative anomalies in the lower stratospheric water vapour and total column ozone at midlatitudes. The anomalies in the water vapour may also be partially attributed to an observed subsidence of the first lapse rate tropopause associated with DTs events. Additionally, the poleward motion of tropical UTLS air with the tropical tropopause overlying the extratropical one must be accompanied by an increase in the frequency of tropospheric intrusions into the lower extratropical stratosphere. This is confirmed by the positive correlation between DTs and ozone laminae found in the HIRDLS data.

The significant anticorrelation between the tropical upwelling and the near global lower stratospheric water vapour is consistent with an uplift of the tropical tropopause accompanying a strengthening of the upward branch of the BDC. A higher tropopause will be colder and drier, leading to negative anomalies in the input of water vapour into the stratosphere. The results are consistent with the findings of Randel et al. (2006) and Randel (2010) which suggest that the decreases in stratospheric water vapour after 2001 is linked to changes in the tropical tropopause and the Brewer-Dobson circulation. In fact, the results here show that the step like decrease in the lower stratospheric water vapour after 2001 is mirrored by a step like increase in the tropical upwelling.

Acknowledgements. We would like to thank William Randel for making water vapour data from the HALOE and Aura MLS available to us. We would like also to thank John Gille, Bruno Nardi and the HIRDLS Team for their efforts in maintaining and continually improving the HIRDLS temperature and ozone data.

ACPD
12, 12391–12421, 2012

This work was partially supported by the DYNOZONE project (PTDC/CTE-ATM/105507/2008) funded by the FCT (Fundação para a Ciência e a Tecnologia, Portugal).

This publication is supported by COST – www.cost.eu

References

Andrews, D. G., Holton, J. R., and Leovy, C. B.: Middle Atmosphere Dynamics, Academic Press, UK, 489 pp., 1987. 12400

Añel, J. A., Antuña, J. C., de la Torre, L., Castanheira, J. M., and Gimeno, L.: Climatological features of global multiple tropopause events, J. Geophys. Res., 113, D00B08, doi:10.1029/2007JD009697, 2008. 12399, 12402

Birner, T.: Recent widening of the tropical belt from global tropopause statistics: sensitivities, J. Geophys. Res., 115, D23109, doi:10.1029/2010JD014664, 2010. 12394

Bönisch, H., Engel, A., Birner, Th., Hoor, P., Tarasick, D. W., and Ray, E. A.: On the structural changes in the Brewer-Dobson circulation after 2000, Atmos. Chem. Phys., 11, 3937–3948, doi:10.5194/acp-11-3937-2011, 2011. 12393, 12398, 12402

Castanheira, J. M. and Gimeno, L.: Association of double tropopause events with baroclinic waves, J. Geophys. Res., 116, D19113, doi:10.1029/2011JD016163, 2011. 12393, 12396, 12397, 12404

Dee, D. P., Uppala, S. M., Simmons, A. J., Berrisford, P., Poli, P., Kobayashi, S., Andrae, U., Balmaseda, M. A., Balsamo, G., Bauer, P., Bechtold, P., Beljaars, A. C. M., van de Berg, L., Bidlot, J., Bormann, N., Delsol, C., Dragani, R., Fuentes, M., Geer, A. J., Haimberger, L., Healy, S. B., Hersbach, H., Hólm, E. V., Isaksen, L., Kållberg, P., Köhler, M., Matricardi, M., McNally, A. P., Monge-Sanz, B. M., Morcrette, J.-J., Park, B.-K., Peubey, C., de Rosnay, P., Tavolato, C., Thépaut, J.-N., and Vtart, F.: The ERA-Interim reanalysis: configuration and performance of the data assimilation system, Q. J. Roy. Meteorol. Soc., 137, 553–597, doi:10.1002/qj.828, 2011. 12394, 12399, 12403

Le Texier, H., Solomon, S., and Garcia, R. R.: The role of molecular hydrogen and methane oxidation in the water vapour budget of the stratosphere, Q. J. Roy. Meteorol. Soc., 114, 281–295, 1988. 12400

ACPD

12, 12391–12421, 2012

Mote, P. W., Rosenlof, K. H., McIntyre, M. E., Carr, E. S., Gille, J. C., Holton, J. R., Kinnersley, J. S., Pumphrey, H. C., Russell, J. M., and Waters, J. W.: An atmospheric tape recorder: the imprint of tropical tropopause temperatures on stratospheric water vapour, J. Geophys. Res., 101, 3989–4006, 1996. 12393, 12400, 12402

Olsen, M. A., Douglass, A. R., Schoeberl, M. R., Rodriquez, J. M., and Yoshida, Y.: Interannual variability of ozone in the winter lower stratosphere and the relationship to lamina and irreversible transport, J. Geophys. Res., 115, D15305, doi:10.1029/2009JD013004, 2010. 12397, 12398

Oman, L., Waugh, D. W., Pawson, S., Stolarski, R. S., Nielsen, J. E.: Understanding the changes of stratospheric water vapour in coupled chemistry–climate model simulations, J. Atmos. Sci., 65, 3278–3291, doi:10.1175/2008JAS2696.1, 2008. 12402

Pan, L. L., Randel, W. J., Gille, J. C., Hall, W. D., Nardi, B., Massie, S., Yudin, V. , Khosravi, R., Konopka, P., and Tarasick, D.: Tropospheric intrusions associated with the secondary tropopause, J. Geophys. Res., 114, D10302, doi:10.1029/2008JD011374, 2009. 12393, 12396, 12398

Peevey, T. R., Gille, J. C., Randall, C. E., and Kunz, A.: Investigation of double tropopause spatial and temporal global variability utilizing high resolution dynamics limb sounder temperature observations, J. Geophys. Res., 117, D01105, doi:10.1029/2011JD016443, 2012. 12393, 12396, 12397, 12398, 12399, 12402, 12404

Randel, W. J.: Variability and trends in stratospheric temperature and water vapour, in: The Stratosphere: Dynamics, Transport and Chemistry, Geophys. Monogr. Ser. 190, AGU, Polvani, edited by: Polvani, L. M., Sobel A. H., and Waugh, D. W., 123–135, doi:10.1029/2009GM000870, Washington, USA, 2010. 12394, 12403, 12404

Randel, W. J., Garcia, R. R., and Wu, F.: Time-dependent upwelling in the tropical lower stratosphere estimated from the zonal-mean momentum budget, J. Atmos. Sci., 59, 2141–2152, 2002. 12400

Randel, W. J., Wu, F., Vomel, H., Nedoluha, G. E., and Forster, P.: Decreases in stratospheric water vapour after 2001: links to changes in the tropical tropopause and the Brewer-Dobson circulation, J. Geophys. Res., 111, D12312, doi:10.1029/2005JD006744, 2006. 12403, 12404

Randel, W. J., Seidel, D. J., and Pan, L. L.: Observational characteristics of double tropopauses, J. Geophys. Res., 112, D07309, doi:10.1029/2006JD007904, 2007. 12393, 12394, 12396

ACPD
12, 12391–12421, 2012

Reichler, T., Dameris, M., and Sausen, R.: Determining the tropopause height from gridded data, Geophys. Res. Lett., 30, 2042, doi:10.1029/2003GL018240, 2003. 12394

Roff, G., Thompson, D. W. J., and Hendon, H.: Does increasing model stratospheric resolution improve extended range forecast skill?, Geophys. Res. Lett., 38, L05809, doi:10.1029/2010GL046515, 2011. 12393

Sigmond, M., Scinocca, J. F., and Kushner, P. J.: Impact of the stratosphere on tropospheric climate change, Geophys. Res. Lett., 35, L12706, doi:10.1029/2008GL033573, 2008. 12393

Solomon, S., Rosenlof, K. H., Portmann, R. W., Daniel, J. S., Davis, S. M., Sanford, T. J., and Plattner, G. K.: Contributions of stratospheric water vapour to decadal changes in the rate of global warming, Science, 327, 1219–1223, doi:10.1126/science.1182488, 2010. 12393

ACPD

12, 12391–12421, 2012

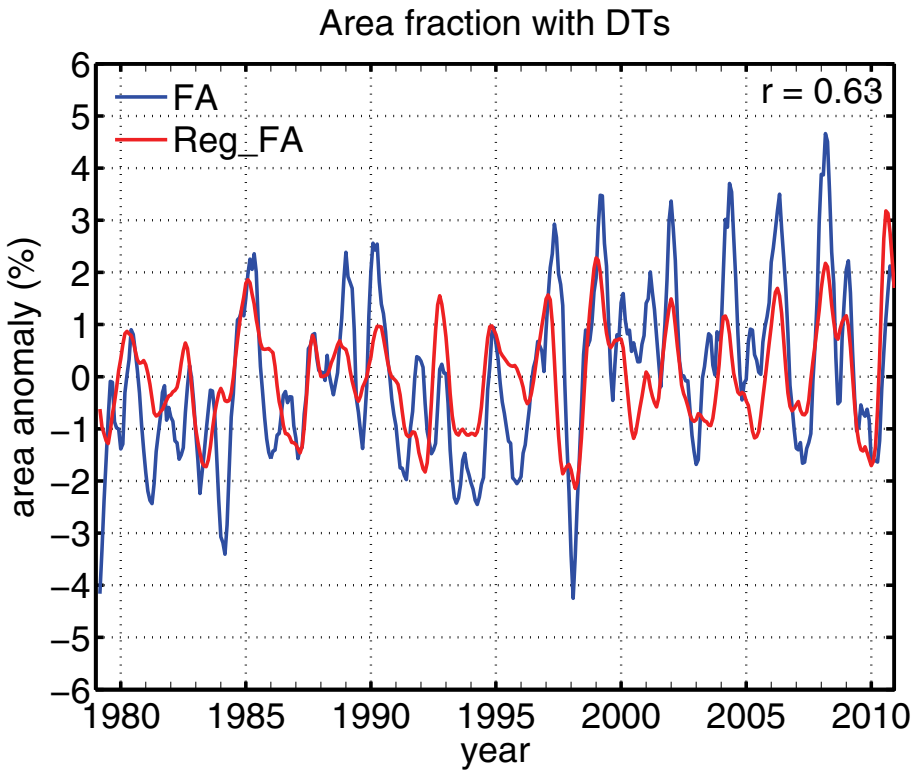

Fig. 1. The blue curve represents the monthly anomalies of the fraction of area (FA) associated with DTs within the 20–65° N and 20–65° S latitude bands. The red curve represents the multilinear regression of the anomalies of FA onto the time series of the QBO, ENSO and solar cycle. Both curves were smoothed by a 5-month running average.

ACPD
12, 12391–12421, 2012

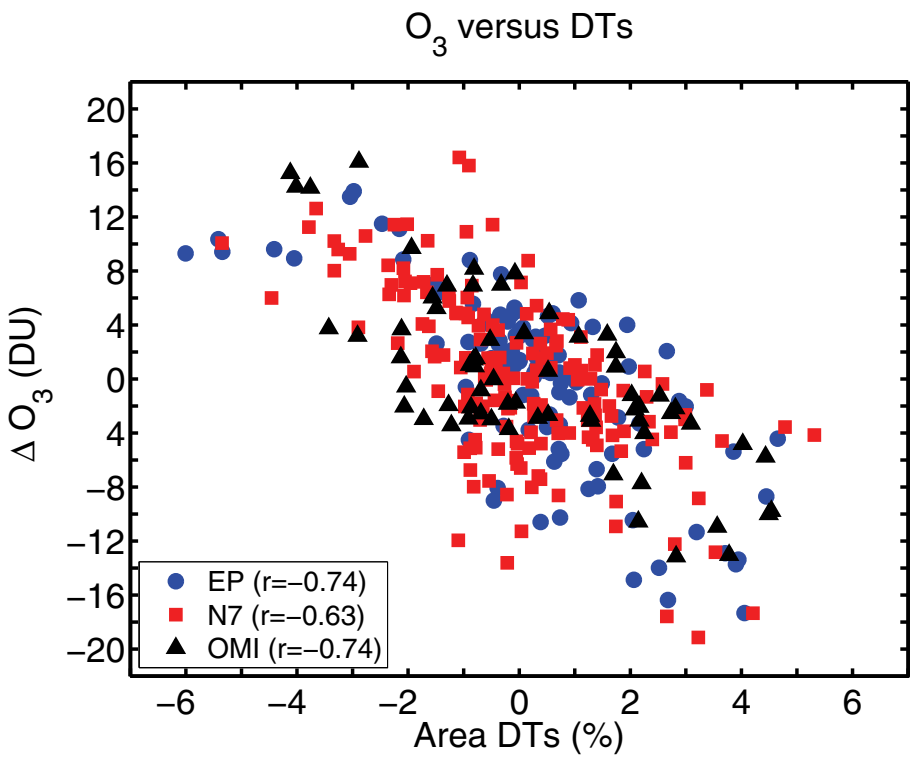

Fig. 2. Anomalies of column ozone in the 30–45° N latitude band as a function of the anomalies of the fraction of area (FA_{NH}) associated with DTs in the NH. The ozone data were derived from three satellite platforms: Earth Probe (EP), Nimbus 7 (N7) and OMI. Using the very conservative assumption that there are only three degrees of freedom per year and for a two-sided test, the correlation for OMI data is statistically significante at the 95 % level, and the correlations for Earth Probe and Nimbus 7 data are statistically significante at the 99 % level.

ACPD
12, 12391–12421, 2012

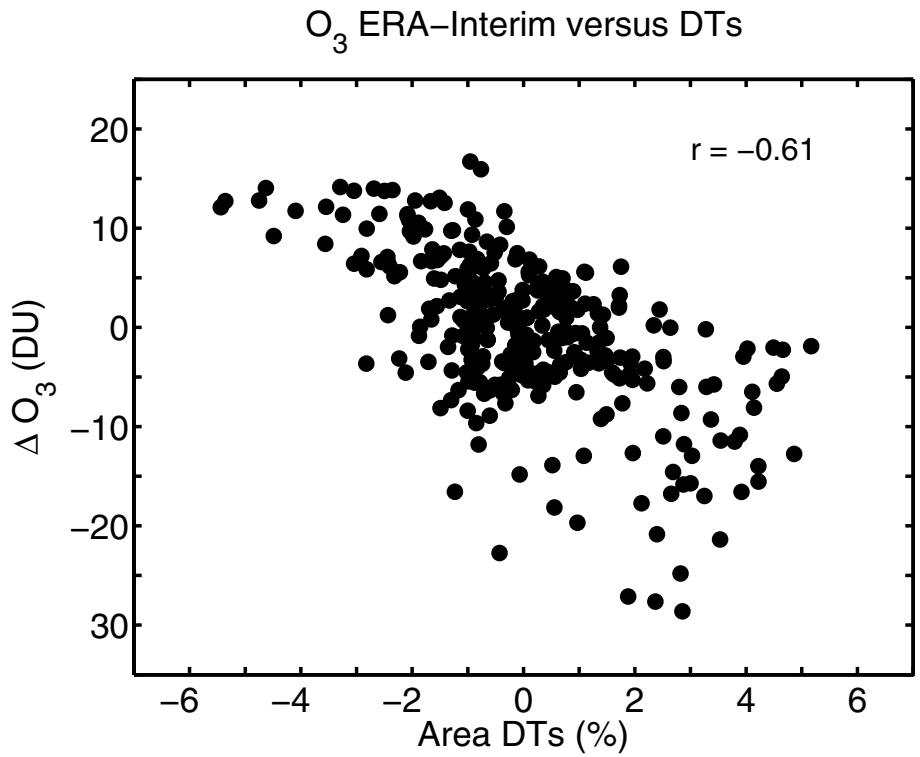

Fig. 3. As in Fig. 2 but with column ozone from ERA Interim reanalysis (1979–2010). A 5-yr running mean was removed to both time series. The correlation is statistical significant at the 99 % level (see the text).

ACPD
12, 12391–12421, 2012

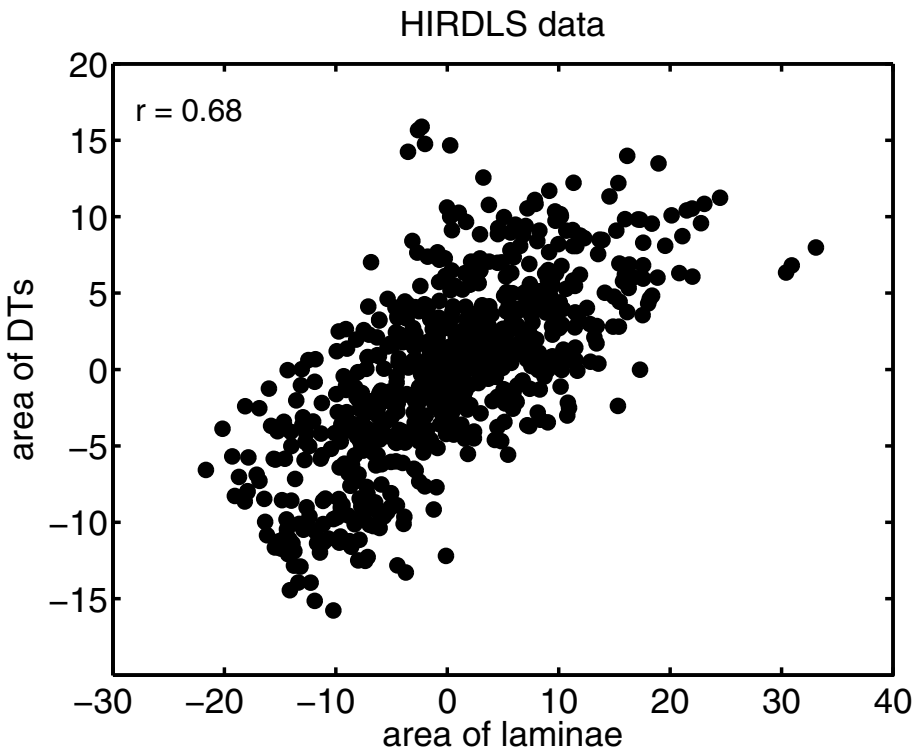

Fig. 4. Correlation between the area covered with DTs and the area covered with ozone laminae in the latitude band (22° N–72° N) as observed by the HIRDLS satellite instruments. Only November to June anomalies are plotted. The correlation is statistically significant at the 99 % level (see text).

ACPD
12, 12391–12421, 2012

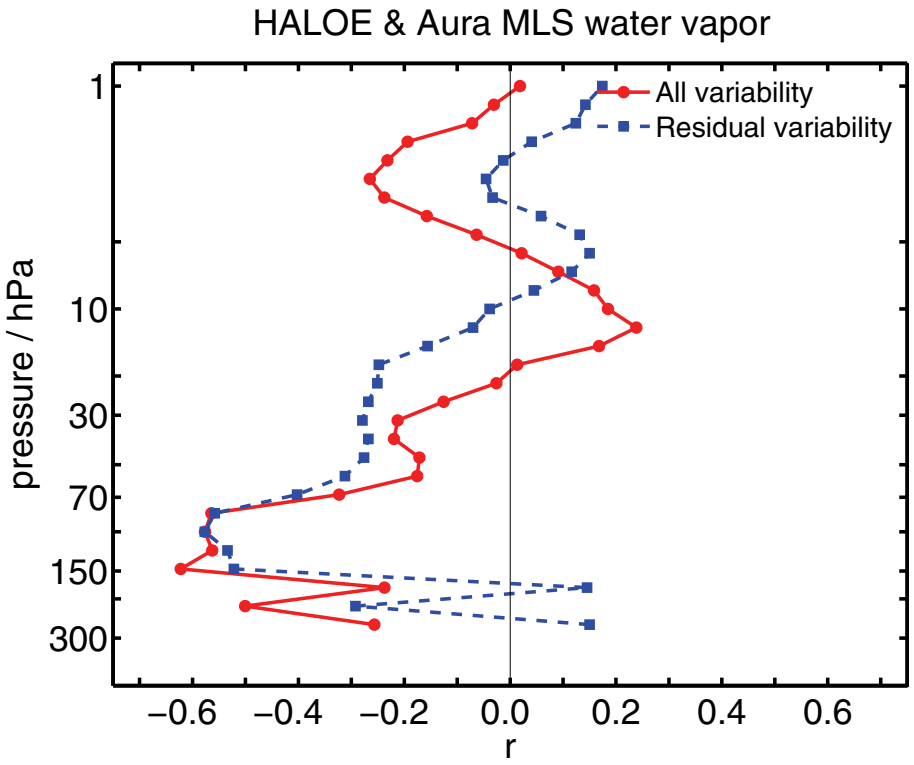

Fig. 5. Correlation between the area covered with DTs, i.e. the time series FA, and the area weighted mean of specific humidity in the latitudinal band (50° S–50° N) derived from the HALOE and Aura MLS instruments. The blue curve shows the correlations between the two time series after the signals of QBO, ENSO and solar cycle have been removed by a multilinear regression. Absolute correlation values greater than 0.3 are statistically significant above the 95 % level (see text).

ACPD
12, 12391–12421, 2012

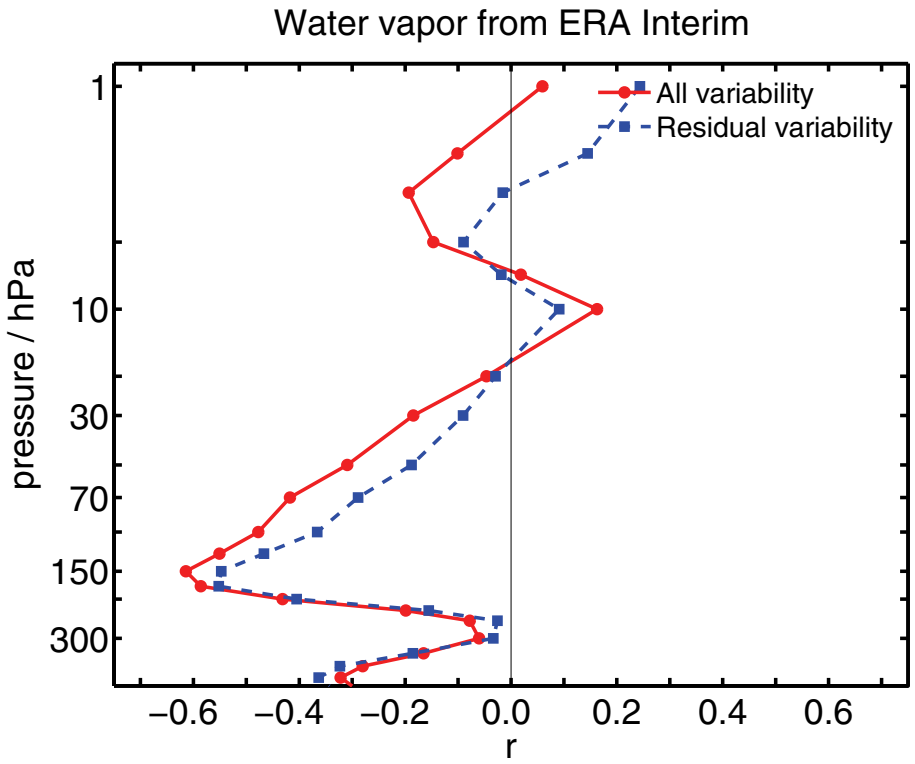

Fig. 6. As in Fig. 5 but using water vapour from the ERA-I reanalysis for the period 1979–2010. Absolute correlation values greater than 0.3 are statistically significant above the 99 % level (see text).

ACPD
12, 12391–12421, 2012

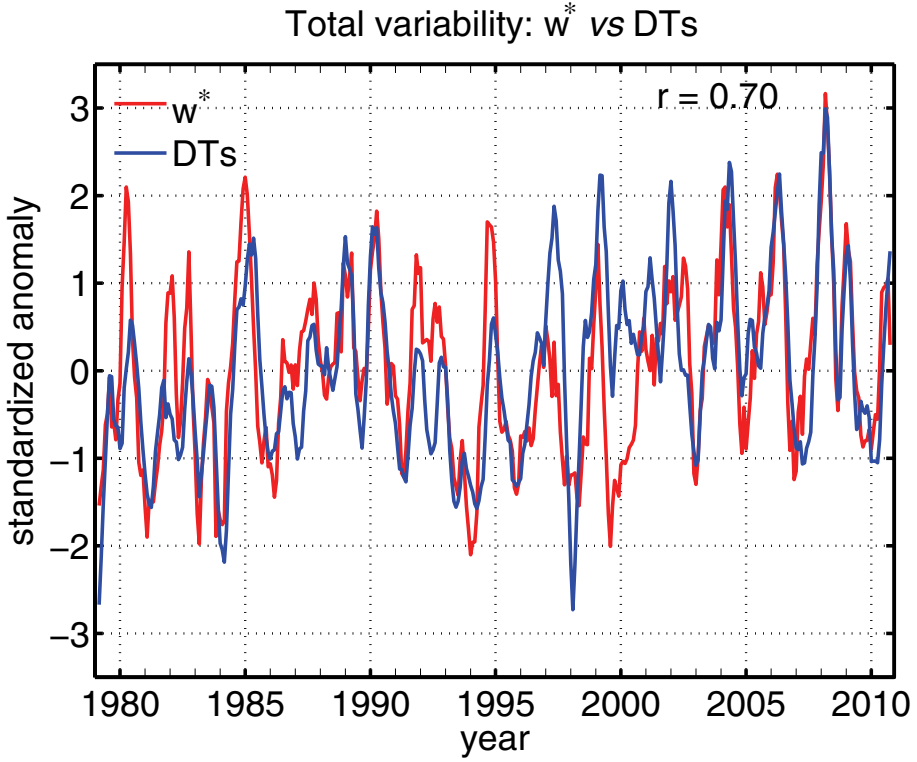

Fig. 7. Time series of mean residual vertical velocity, $\langle \overline{w^*} \rangle$, in the tropics (22.5° S–22.5° N) and of the fraction of area covered with DTs derived from ERA-I reanalysis. Both time series were smoothed by a 5-month running mean and normalized by their respective standard deviations.

ACPD
12, 12391–12421, 2012

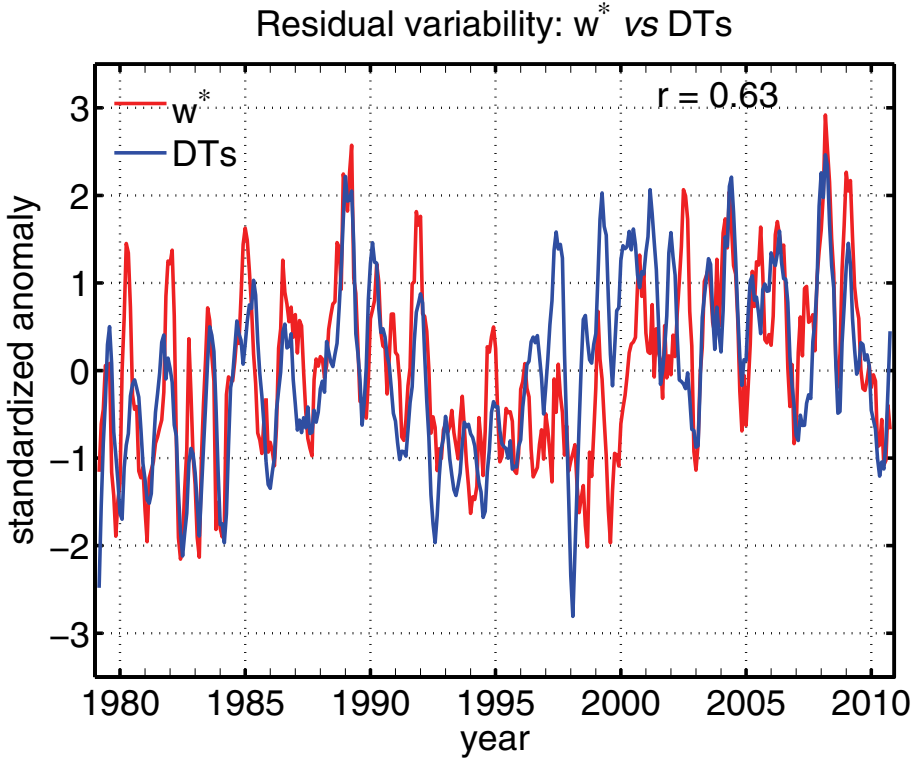

Fig. 8. As in Fig. 7 but with the linear components of the QBO, the ENSO and the solar cycle removed from both time series.

ACPD
12, 12391–12421, 2012

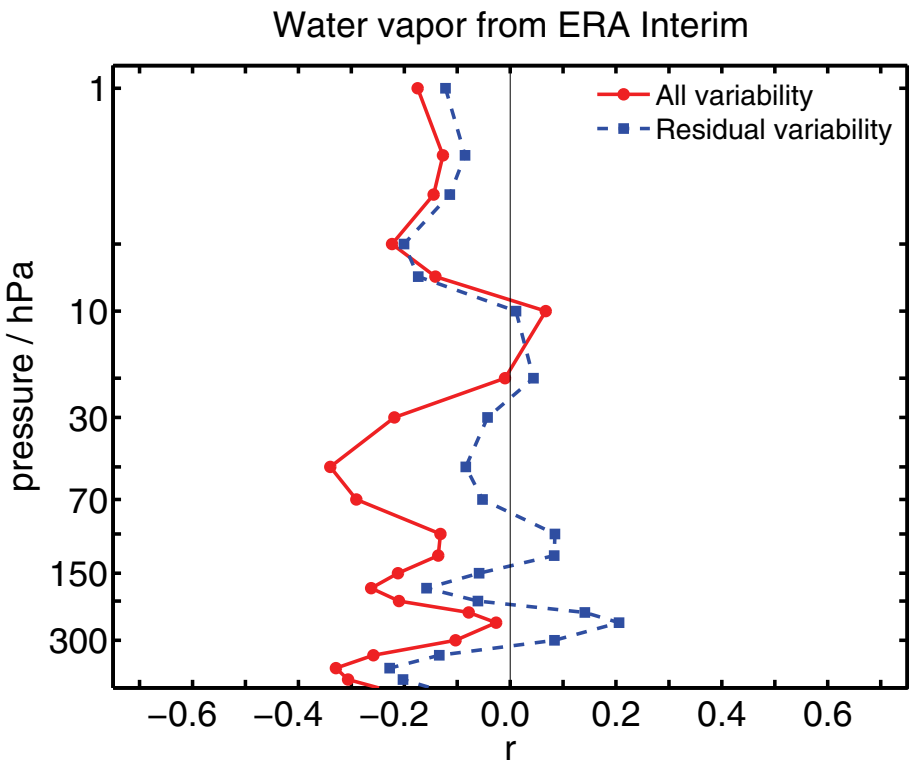

Fig. 9. Correlation between the tropical upwelling and the area weighted mean of ERA-I specific humidity in the latitudinal band (50° S–50° N) with the tropical upwelling leading by 5 months (see text). Both time series were smoothed by a 5-month running mean. The blue curve shows the correlations between the two time series after the signals of QBO, ENSO and solar cycle have been removed by a multilinear regression.

ACPD
12, 12391–12421, 2012

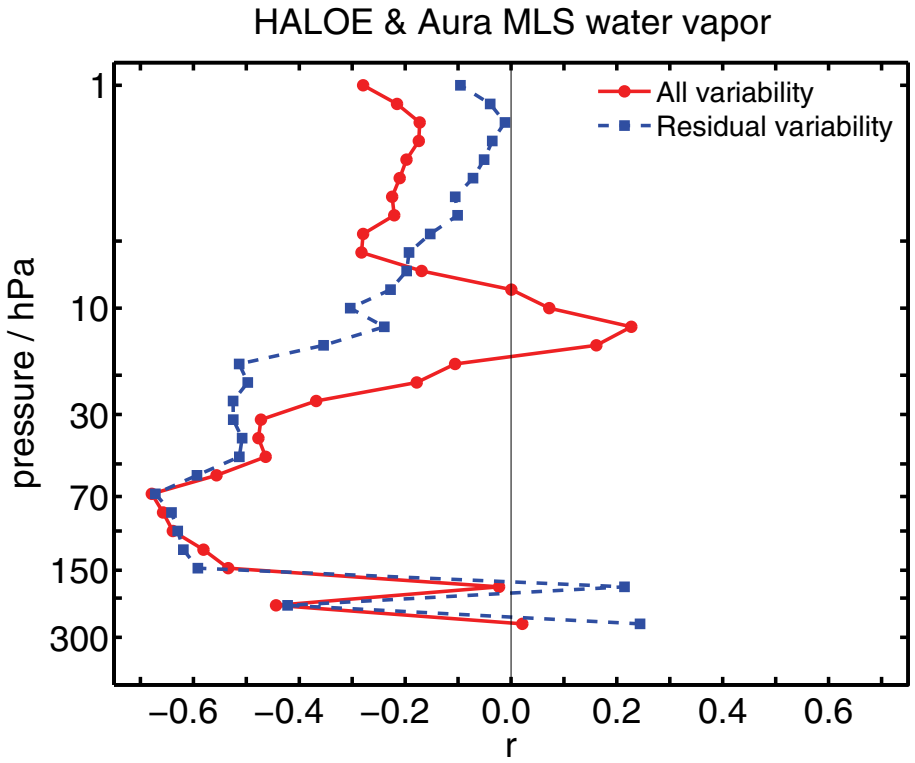

Fig. 10. As in Fig. 9 but with the area weighted mean of the water vapour mixing ratio within the latitudinal band (50° S–50° N) derived from the HALOE and Aura MLS instruments. Absolute correlation values greater than 0.3 are statistically significant above the 95 % level.

ACPD
12, 12391–12421, 2012

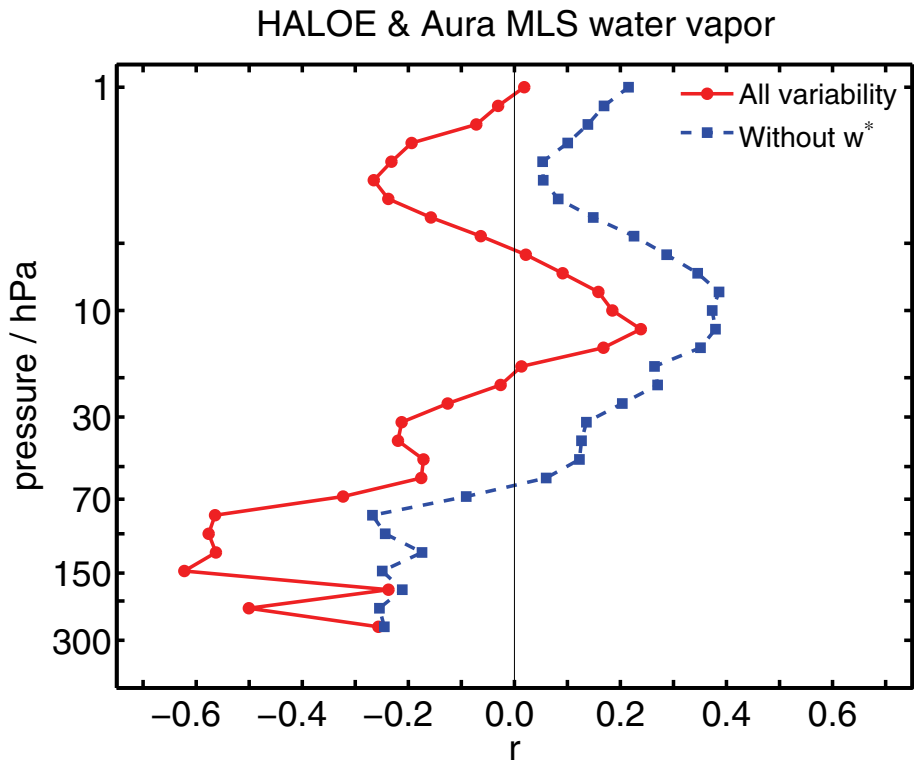

Fig. 11. Correlation between the area covered with DTs and the area weighted mean of the water vapour mixing ratio within the latitudinal band (50° S–50° N) derived from the HALOE and Aura MLS instruments. The blue curve shows the correlations between the two time series after subtracting the variabilities regressed on the tropical upwelling time series.

ACPD
12, 12391–12421, 2012

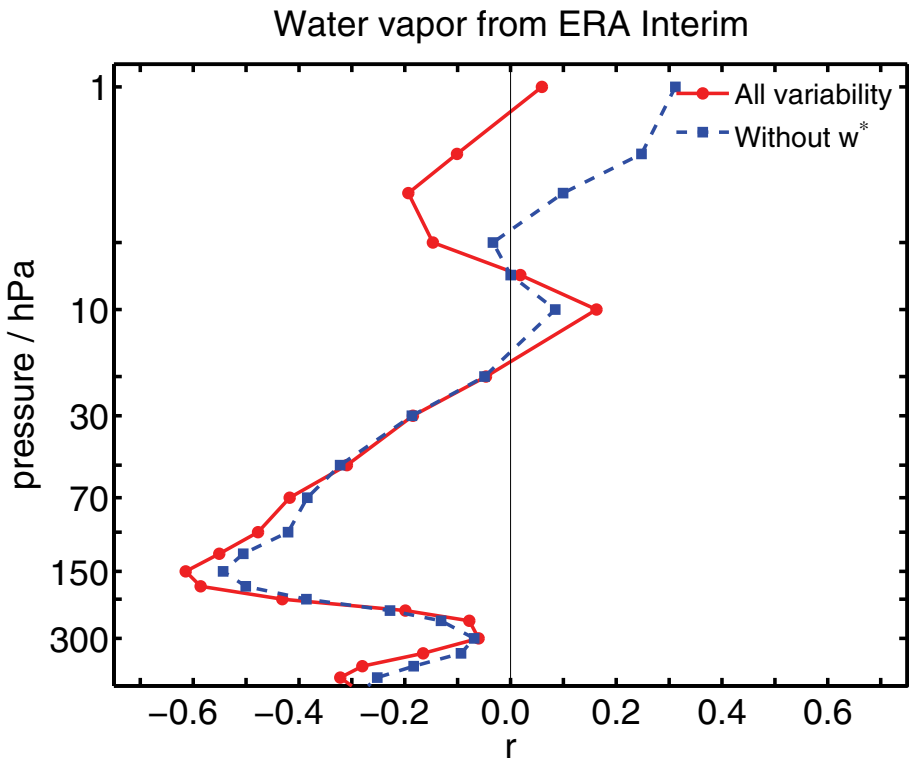

Fig. 12. As in Fig. 11 but with ERA interim water vapour data.

ACPD
12, 12391–12421, 2012

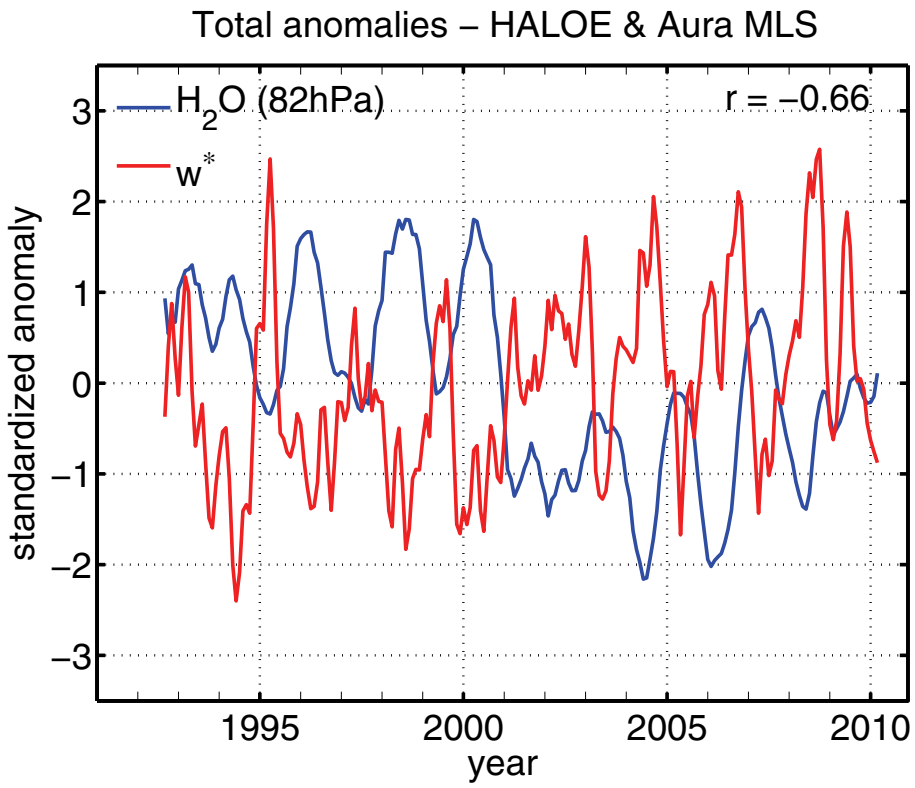

Fig. 13. Time series of mean residual vertical velocity, $\langle \overline{w}^* \rangle$, in the tropics (22.5° S–22.5° N) and the near-global (50° S–50° N) water vapour anomalies at 82-hPa. The water vapour data were derived from the HALOE and Aura MLS instruments. Both time series were smoothed by a 5-month running mean and normalized by their respective standard deviations. The time series of the residual vertical velocity leads the water vapour by 5 months. This means that time series of the vertical velocity was shifted five months to the left in the plot.

ACPD
12, 12391–12421, 2012

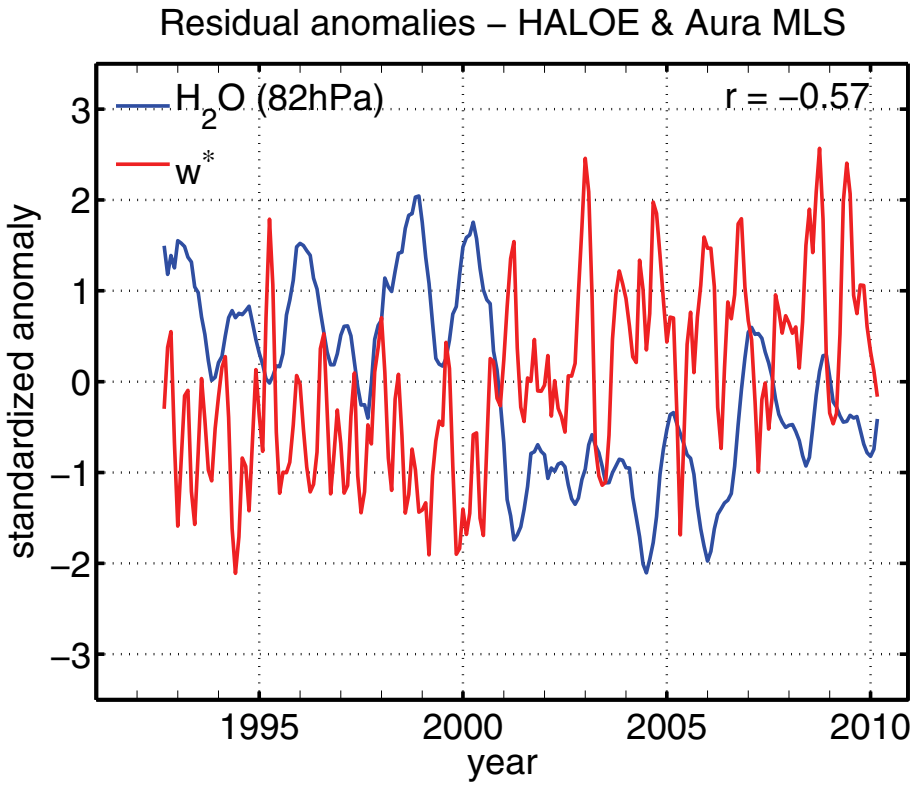

Fig. 14. As in Fig. 13 but with the linear components of the QBO, the ENSO and the solar cycle removed from both the time series.

ACPD
12, 12391–12421, 2012